Electronic and structural analysis of Sb-induced GaAs(100)(2×4) and (2×8) surfaces

P. Laukkanen,* R. E. Perälä, R.-L. Vaara, and I. J. Väyrynen
Department of Physics, University of Turku, FIN-20014 Turku, Finland

M. Kuzmin
A. F. Ioffe Physico-Technical Institute, Russian Academy of Sciences, St. Petersburg 194021, Russian Federation

J. Sadowski
MAX-lab, Lund University, SE-221 00 Lund, Sweden
and Institute of Physics, Polish Academy of Sciences, al. Lotnikow 32/46, 02-668 Warszawa, Poland
(Received 23 April 2003; revised manuscript received 19 December 2003; published 28 May 2004)

Electronic and structural properties of Sb-induced GaAs(100)(2×4) and (2×8) surfaces are studied by means of core-level and valence-band photoelectron spectroscopy utilizing synchrotron radiation and scanning tunneling microscopy. Combining these results and showing good consistency among them, we demonstrate that the Sb/GaAs(100)(2×4) surface is well compatible with the δ structural model, which includes one Sb dimer in both the first and third atomic layers and two second-layer Ga dimers per unit cell (i.e., the Sb coverage of 0.5 ML), giving experimental support to generality of the δ-type model for $III-V(100)(2\times4)$ surfaces, proposed previously on the basis of *ab-initio* calculations. Deconvolution of the Sb $4d$ core-level spectrum from the (2×4) surface shows two components, which are tentatively connected to two inequivalent Sb-dimer sites in the δ unit cell. Angle-resolved valence-band photoelectron spectroscopy reveals Sb-induced surface-derived states at near 0.4 and 0.6 eV below the valence-band maximum (VBM) for the Sb/GaAs(100)(2×4) surface, which have not been found in earlier measurements. These two surface-derived features mapped along symmetry lines of the surface Brillouin zone are identified with previous electronic-structure calculations. The results are also compared to band-structure measurements of the As/GaAs(100) ×(2×4) surface found in the literature. For the Sb/GaAs(100)(2×8) surface, we propose a structural model which, in contrast to the recent model, obeys the electron counting rule and consists of Sb dimers in three atomic layers, showing the Sb coverage of 1.25 ML for the (2×8) surface. The Sb $4d$ core-level spectrum from this surface exhibits three components, which are discussed within the determined structural model. The valence-band measurements of the (2×8) surface propose a new Sb-induced surface state at near 0.5 eV below the VBM.

DOI: 10.1103/PhysRevB.69.205323 PACS number(s): 73.20.At, 68.43.Fg, 68.37.Ef

I. INTRODUCTION

The surface formed by adsorption of the group-V element of Sb on GaAs(100) is interesting from both scientific and technological viewpoints. First, such an interaction of the semiconductor surface with adsorbate atoms can give insight into physics and chemistry of the surface itself, and also into the bonding character of the group-V elements on $III-V(100)$. Understanding of the group-V elements bonding to $III-V$ semiconductor surfaces is essential for realizing initial stages of epitaxial growth of these compounds (see Refs. 1 and 2 for example). Among compound semiconductors, GaAs(100) is the most utilized substrate in device applications which typically consist of a multilayer structure grown epitaxially on the GaAs(100) surface. Furthermore, an Sb-terminated GaAs(100) surface, as such, represents the initial face for the $III-V$-based heteroepitaxy. The ordered Sb/GaAs(100) surfaces provide thus a good starting point for studying the electronic and geometrical properties of the surfaces and adsorbate layers which also have potential applications in electronics and optoelectronics.

Although Sb/GaAs(100) has been the subject of theoretical and experimental investigations for several decades,[3] more attention has been paid to the adsorption of Sb and other group-V elements (e.g., As, Bi) on nonpolar GaAs(110) as well as other $III-V(110)$ surfaces.[4–10] These adsorbate layers have been shown to form an ordered (1×1) structure on the (110) face at the coverage of about one monolayer (ML), which has enabled the detailed electronic and structural studies of the overlayers and interfaces and further investigations of universality of the models shown for these $III-V(110)$ systems.

In contrast to $III-V(110)$, the $III-V(100)$ surfaces show a variety of reconstructions that differ in symmetry and stoichiometry.[11,12] Among them the (2×4)-reconstructed $III-V(100)$ surface is an especially interesting one because it is typically observed in molecular-beam epitaxy (MBE) growth of GaAs- and InP-based compounds under a wide range of growth conditions on the (100) face. The As-stabilized GaAs(100)(2×4) surface is extensively studied, and its three stable phases, i.e., α, $\beta2$, and γ, are well established. The α phase consists of two As dimers in the top layer and two second-layer Ga dimers per (2×4) unit cell, and its surface As coverage is 0.5 monolayer (ML). The $\beta2$ is a more As-rich phase (0.75 ML of As) showing two As dimers in the top layer and one As dimer in the third layer per unit cell. The γ one is merely a mixture of the $\beta2$ and As-super-rich $c(4\times4)$ phases. The As coverage of the c(4

 ©2004 The American Physical Society

$\times 4)$ surface has been found to be 1.0–1.75 ML.[13] The GaAs(100) surface structures have been considered as model systems for many $III-V(100)$ surfaces, however, more recent investigations have questioned the generalization of the α model for the less group-V rich (2×4) surfaces. Total-energy calculations for GaP and InP(100) have revealed that a $(2\times4)\,\delta$ model, which consists of one P dimer in both the top and third atomic layer and two group-III dimers in the second layer per unit cell (the group-V coverage of 0.5 ML), is more stable than the α one irrespective of the surface chemical potentials.[14] Likewise, total-energy calculations for the GaAs$(100)(2\times4)$ surface have also shown the δ model to be more favorable than the α one,[15] and recently, calculations combined with STM measurements of InAs$(100)(2\times4)$ have verified the $\beta2$ and δ models to be correct for that surface.[16]

Investigations of GaAs$(100)(2\times4)$ surfaces stabilized by V-group elements, like Sb, can provide additional information on these structural models and their generality. Maeda *et al.*[17] have studied the Sb/GaAs$(100)(2\times4)$ surface by reflection high-energy electron diffraction (RHEED) and core-level photoelectron spectroscopy. They have found that the Sb/GaAs(100) surface with a (2×4) RHEED pattern, which was observed after annealing the surface at 440–560 °C, is terminated by Sb and that the reconstruction changes involve As atom desorption followed by Sb atom substitution (i.e., As-Sb exchange). An interesting point is that those Sb $4d$ core-level studies have shown only one bonding environment for Sb atoms on this (2×4) surface, but two surface-related contributions have been found in the As $3d$ spectrum from the As/GaAs$(100)(2\times4)$ surface.[18–20] In further investigations, the atomic structure of the Sb/GaAs$(100)(2\times4)$ surface has been studied by x-ray standing wave (XSW),[21,22] scanning tunneling microscopy (STM),[23,24] and reflectance anisotropy spectroscopy (RAS).[25] Moriarty *et al.*[23] have proposed the δ model for Sb/GaAs$(100)(2\times4)$, where the top-layer As dimer is replaced by Sb dimer. Afterwards, the structural studies of the Sb/GaAs$(100)(2\times4)$ surface have stated the α and $\beta2$ phases, supporting the established (2×4) models,[22,25] and a new β-like structure with the unit cell of one As and two Sb dimers in the top layer.[24] However, *ab initio* calculations of the Sb/GaAs$(100)(2\times4)$ have revealed three stable phases, namely, $\beta2$, δ_1, and δ_2, to be most favorable.[26] In the Sb/GaAs$(100)(2\times4)\beta2$ model, all the top and third-layer As dimers are substituted by the Sb ones, i.e., Sb surface coverage is 0.75 ML. For the lower Sb amounts, the most favorable models were proposed to be the δ_1 structure presented originally by Moriarty *et al.* and the δ_2 one, where the third-layer As dimer of δ_1 is also replaced by a Sb dimer. Calculations have also revealed that the surface-electronic structure of Sb/GaAs$(100)(2\times4)$ is similar to that of the As/GaAs$(100)(2\times4)$ surface,[26] which can be expected because of their similar geometrical arrangements and the chemical similarity of the both group-V elements. It is surprising that the positions of the highest surface states for the calculated Sb and As/GaAs$(100)(2\times4)$ surfaces are nearly identical although the orbital energies of As and Sb valence electrons are different. This is shown to arise from the shorter As-dimer bond length.[26] However, these calculated Sb-induced surface states have not been found in previous valence-band measurements,[27] and it is still unclear which models are correct for Sb/GaAs$(100)(2\times4)$.

From these perspectives, we have performed the analysis of the chemical, electronic, and structural properties of the Sb/GaAs$(100)(2\times4)$ surface utilizing core-level and valence-band photoelectron spectroscopy and STM measurements. Combining these results and showing good consistency among them, we demonstrate the Sb/GaAs$(100)(2\times4)$ surface to be well consistent with the δ_2 model. Deconvolution of Sb $4d$ core-level spectrum from this (2×4) surface shows two components, which are tentatively connected to two inequivalent Sb dimers in the δ_2 unit cell. Our angle-resolved photoelectron spectroscopy (ARPES) measurements from this surface show two new Sb-induced surface states, in consistency with theory. These surface-related spectral features are identified by the comparison with the previous calculations.[26] It is also instructive to compare the valence-band measurements with previous electronic-structure results of the As/GaAs$(100)(2\times4)$ surface.[28]

To further our knowledge about the interaction of the Sb overlayer with a GaAs(100) surface and the effects of the Sb bonding geometry on the surface-electronic structure, we study the Sb-terminated GaAs$(100)(2\times8)$ surface that is observed at the higher Sb coverage ($\sim$1 ML). Taking into account an absence of reports on the $c(4\times4)$ structure of Sb/GaAs(100) in literature, one can expect that the Sb/GaAs(100) surface exhibits the (2×8) rather than $c(4\times4)$ periodicity at higher coverages. This expectation is also supported by observations of the present work. It is important to emphasize here that the $c(4\times4)$ reconstruction has been commonly observed on III-As and III-Sb(100) surfaces at the monolayer coverages and in the MBE growth of these compounds under the most As- and Sb-rich growth conditions, respectively, while the Sb/GaSb(100) surface does not form the $c(4\times4)$ structure but instead exhibits the chainlike (2×10) and $c(2\times10)$ reconstructions.[29–31] Thus, the latter can be considered as an important exception among the III-As and III-Sb(100) surfaces, and some characteristics of the interaction between the Sb layer and the GaSb(100) surface can tentatively apply also for the Sb/GaAs(100) system at the monolayer coverages. The Sb/GaAs$(100)(2\times8)$ structure has been found only recently and less is known about the properties of this surface. Maeda and Watanabe have shown that the Sb $4d$ core level of Sb/GaAs$(100)(2\times8)$ consists of three components and that more of the Sb atoms on this (2×8) surface are bonded to Sb atoms than to Ga atoms.[32] Whitman *et al.*[24] have investigated Sb/GaAs$(100)(2\times8)$ by STM and proposed a model showing a chainlike multilayer structure with $\sim$1 ML of Sb, which is locally identical to the Sb/GaSb(100) surfaces. This local similarity is also supported by our measurements, but the present results are not fully consistent with the previous ones, and we propose a new model for Sb/GaAs$(100)(2\times8)$.

II. EXPERIMENTAL

Photoemission experiments were carried out at the Swedish National Synchrotron Radiation Center, MAX-lab, on the

toroidal grating monochromator beam line 41 at the MAX I storage ring using p-polarized light for excitation. The photon energy was 90 eV and the light incidence angle 45° relative to the surface normal. To vary a surface sensitivity to As $3d$, Ga $3d$, and Sb $4d$ core-level photoelectrons, the takeoff angles of 0° and 60° from the surface normal were used. The photoemission spectra were taken using a hemispherical electron energy analyzer with an angular resolution of $\sim 2°$ and a total energy resolution better than 0.3 eV. Spectra in the valence-band region were obtained with the photon energy of 21 eV.

RHEED observations were done in the MBE system connected to the analysis chamber of the 41 beam line. Substrates were cut from n-type ($n \sim 1 \times 10^{18}$ cm^{-3}) GaAs(100)$\pm$0.1° wafers and they were attached on Mo holders by In. The surface oxides were removed by thermal annealing at 620 °C in As_2 flux. A substrate temperature was monitored by an infrared pyrometer. Undoped GaAs buffer layers were grown at 580 °C under As-rich (2×4) conditions. After the growth of the GaAs buffer, the Ga shutter was closed and the surface was annealed at the growth temperature under the same As flux for 10 s. A sharp (2×4) RHEED pattern, which resembled a pattern of the (2×4)β2 phase,[12] maintained indicating the well ordered surface. This was a starting face for the preparation of a Sb-induced reconstruction.

Then the Sb shutter was opened and a group-V soak of Sb_4 (0.04 ML/s) and As_2 was supplied to the (2×4) surface at 580 °C for 10 s. Upon that the As flux was terminated and the substrate was slowly cooled down to 450 °C in 20 minutes under the Sb flux to get the Sb-terminated (2×8) surface monitored by RHEED. The sharp (2×4) RHEED pattern remained when the Sb shutter was opened. Integral and fractional order streaks of the (2×4) pattern in the [0–11] azimuth became broader with the evaporation time of Sb_4 and decreasing the substrate temperature. Below 500 °C the (2×4) pattern gradually disappeared, and a (2×8) diffraction pattern loomed up. The surface was exposed in Sb_4 at 450 °C for 5 min at which the (2×8) RHEED became sharp. It is worth mentioning that apart from (2×4) and (2×8), no other Sb-induced pattern was observed during the experiments among several samples. After closing the Sb flux, the samples were treated as the following three cases.

Sample A was reheated up to 580 °C without the Sb flux. The (2×8) RHEED changed gradually to a (2×4) pattern with the temperature, and the sharp (2×4) RHEED was observed at $\sim$550 °C.

Sample B was cooled to around 200 °C and kept therein for 15 min to avoid unintentional As or Sb adsorption on the surface in MBE and cooled down to room temperature. The clear (2×8) RHEED was retained through the cooling to room temperature. Then it was transferred into the analysis chamber under vacuum conditions and checked by low-energy electron diffraction (LEED), which showed a low-background (2×8) pattern for this surface. The sample was rotated to keep the [0–11] or [011] azimuth in the plane of incidence for the valence-band measurements. A clear (2×4) LEED pattern was obtained when the (2×8) surface was heated up to 550 °C in the analysis chamber. The sample temperature was measured by an infrared thermometer. The quality of RHEED and LEED patterns showed that the ordered (2×4) and (2×8) surfaces were obtained by the above procedures. We note in passing that similar procedures have been previously used to prepare ordered Sb/GaAs(100)(2×4) and (2×8) surfaces.[24]

Sample C, As-capped, was prepared for STM experiments which were performed in another vacuum system. An arsenic capping layer was used to protect the Sb-terminated GaAs surface against air exposure during shipping between the laboratories. When the Sb-induced GaAs(100)(2×8) surface was prepared in MBE, as described above, it was allowed to cool to room temperature and then exposed to an As_2 flux for 25 min. Once inside the other vacuum system, the As capping layer was removed by heating the sample first at 200 °C for $\sim$12 h and then carefully increasing the temperature up to 550 °C. When the sample was cooled down, it was checked with LEED before STM experiments. Both LEED and STM showed the (2×4) reconstruction for this surface (Sec. III B). To produce the Sb-induced (2×8) surface for STM, Sb was evaporated on the heated (2×4) surface from a tungsten coil evaporator with flux of 0.02 ML/s for $\sim$30 min while simultaneously decreasing the sample temperature slowly from 550 to 450 °C. LEED and STM confirmed (2×8) reconstruction (Sec. III B). The reheating of the (2×8) surface at 550 °C, as performed with Sample B, produced the (2×4) reconstruction similar to that found after the decapping of this sample at 550 °C, showing that the decapped surface was Sb-terminated. The clear (2×4) and (2×8) LEED patterns were similar to those observed with the photoemission measurements. Omicron STM was used in the constant current mode with a tunneling current of 0.08–0.3 nA and a sample bias voltage of -3.5 to 3.5 V.

Here, we discuss the fact that the starting surface and As-background conditions in the preparation of the Sb-terminated (2×8) surface using MBE for the photoemission measurements were different from those for the STM experiments. An essential point is the presence of arsenic on the surface [i.e., the As/GaAs(100)(2×4)β2 surface] when the Sb evaporation was started in MBE with the photoemission experiments. For STM, the Sb/GaAs(100)(2×4)δ_2 surface (Sec. III B) was the starting point. However, these differences in the preparation conditions do not affect significantly on the final (2×8) structure because the substrate temperature was high (550–580 °C) in the beginning of the Sb evaporation and the following substrate cooling was slow. At such an elevated temperature, the stability of Sb layer is much higher than that for As overlayer.[33,34]

III. RESULTS AND DISCUSSION

A. Core-level photoemission

The As $3d$, Ga $3d$, and Sb $4d$ core-level spectra from the Sb/GaAs(100)(2×4) and (2×8) surfaces were analyzed by fitting the spectra to a linear combination of Voigt line shapes using standard methods. The background of the spectra was subtracted applying Shirley's method. The fitting parameters,

TABLE I. Fitting parameters for the As $3d$, Ga $3d$, and Sb $4d$ core-level spectra from Sb-induced GaAs(100)(2×4) and (2×8) surfaces. Binding-energy (BE) shifts of the As and Ga surface components are referenced to the GaAs bulk components (B) and the shifts of the Sb components to the $S1$. The "−" sign indicates a shift toward lower BE. The relative intensities of the surface components are determined from the spectra obtained at the 60° and normal emission. All energies are in eV.

	As $3d$	Ga $3d$	Sb $4d$
Spin–orbit splitting	0.68	0.45	1.243
Branching ratio	0.64±0.01	0.66±0.01	0.69±0.01
Lorentzian width	0.16	0.16	0.16
Gaussian width	0.48	0.39	0.52
The (2×4) surface:			
BE shift of $S1$*		−0.25	
BE shift of $S2$*		0.36	0.44
$S1^*/B$@60° (normal)		0.53 (0.34)	
$S2^*/B$@60° (normal)		0.46 (0.29)	
$S1^*/S2^*$@60° (normal)		1.15 (1.17)	0.92 (1.01)
The (2×8) surface:			
BE shift of $S1$	−0.39	−0.39	
BE shift of $S2$	0.57	0.27	0.59
BE shift of $S3$			1.07
$S1/B$@60° (normal)	0.45 (0.23)	0.37 (0.38)	
$S2/B$@60° (normal)	0.21 (0.22)	0.47 (0.31)	
$S1/S2$@60° (normal)	2.14 (1.05)	0.79 (1.23)	1.04 (1.20)
$S1/S3$@60° (normal)			1.11 (1.90)

relative binding energies, and intensity ratios for the components of the As, Ga, and Sb core spectra are listed in Table I. A binding energy (BE) scale was fixed setting the Ga $3d_{5/2}$ bulk component at 18.60 eV, referred to as the valence-band maximum,[35] and the binding energies of the As and Sb peaks were set using the corrections from the Ga $3d$ spectra. The core-level spectra are rather featureless in the present work, and it is well known that the fitting of such spectra is not unique. Therefore, we shortly describe our data processing. To obtain some confidence in a number of the components (i.e., spin–orbit doublets) involved in the spectra, it is necessary to determine the component width justifiably. The energy-broadening parameters were required to comply with the instrumental resolution (Gaussian shape) and lifetime widths (Lorentzian shape). At first, Lorentzian widths as well as spin–orbit splittings and branching ratios were fixed (Table I), while Gaussian broadening was allowed to vary. When the Gaussian widths, which were retained constant throughout the different Sb coverages and emission angles among several samples, were concluded, they were also fixed. The remaining parameters, i.e., a number of the components and their binding energies and relative intensities, were obtained as a result of the fitting process. As seen in Table I, the instrumental width (<0.3 eV) is smaller than the deduced Gaussian widths, agreeing with previous studies of many $III-V$ surfaces with similar instrumental resolution.[19,20,29,36,37] Also, the full widths (FWHM) of the present components are consistent with previous ones.[18,32,35,38]

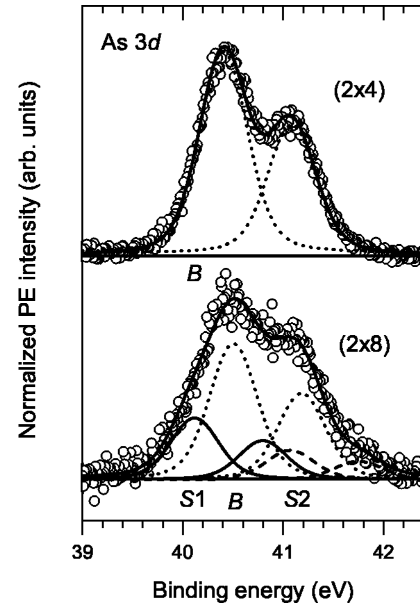

FIG. 1. The As $3d$ core-level spectra, spin–orbit doublets of fitting, and the result of the fit (the solid line through the data points) for the Sb/GaAs(100)(2×4) and (2×8) surfaces. The fitting parameters are listed in Table I.

The As $3d$ core-level spectrum at the emission angle of 60° for the Sb/GaAs(100)(2×8) surface shown at the bottom of Fig. 1 exhibits the presence of the GaAs bulk component B and two shifted components $S1$ and $S2$ at the lower and higher binding-energy side of the bulk component, respectively. This spectrum is qualitatively similar to those measured previously from GaAs(100) reconstructions,[18–20,38,39] of which spectra consist of the two shifted components besides the bulk one. The appearance of the two shifted As components indicates that the (2×8) surface involves As atoms of which chemical environments are different from the GaAs bulk atoms. This is tentatively consistent with previous Sb/GaAs(100)(2×8) studies that have proposed the presence of As dimers on that surface structure.[24] Another origin for these surface-related As components can arise from a patchy Sb layer on the surface, i.e., there are Sb vacancies on the (2×8) surface. We associate $S2$ with group-V–group-V bonding (As-As and/or As-Sb).[38,39] In contrast to $S1$, whose intensity decreases at the normal emission (Table I), we find that the intensity ratio $S2/B$ remains in less surface sensitive conditions at the normal emission (not shown) indicating that the origin of $S2$ is related to subsurface As atoms rather than As site on the (2×8) surface.

The upper panel of Fig. 1 shows the As $3d$ spectrum at 60°-emission from the Sb/GaAs(100)(2×4) surface obtained by heating the (2×8) surface at 550 °C. No surface components, such as the $S1$ or $S2$, were resolved, within detection limits, from the (2×4) surface and only the fourfold-coordinated bulk component was observed. This indicates that As atoms remain no longer on the Sb/GaAs(100)(2×4) surface due to the high temperature, at which As atoms can easily desorb. We note also that the

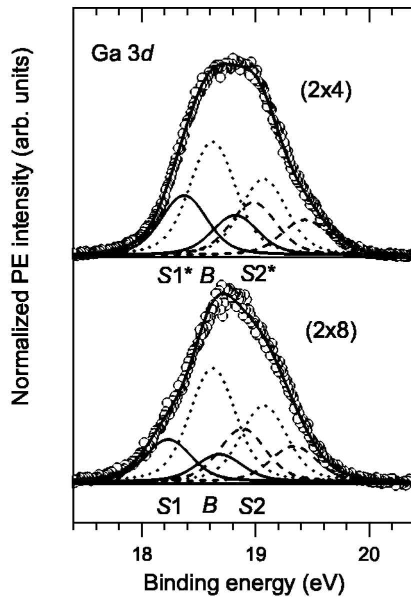

FIG. 2. The same as Fig. 1 but for Ga $3d$ core-level spectra.

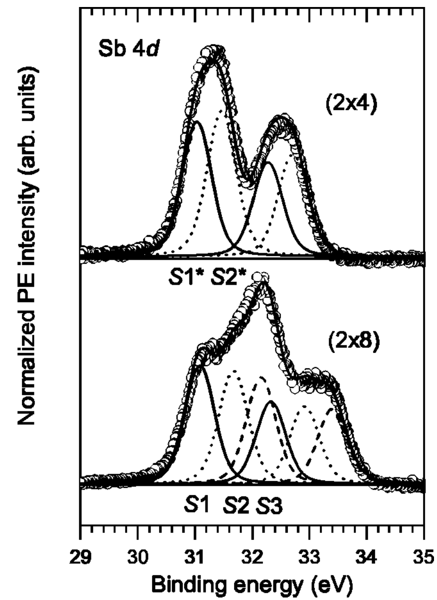

FIG. 3. The same as Fig. 1 but for Sb $4d$ core-level spectra.

normal-emission spectrum (not shown) is qualitatively very similar to that at the 60°-emission, supporting the absence of the As surface components.

Figure 2 shows the Ga $3d$ core spectra of the Sb/GaAs(100)(2×4) and (2×8) surfaces at the 60°-emission. In addition to the bulk component B, the low ($S1^*$ or $S1$) and high ($S2^*$ or $S2$) BE-side components are observed in both spectra. The components $S1$ ($S2$) and $S1^*$ ($S2^*$) are denoted as two different components because of their different BE separations from B. The both high BE-side features $S2$ and $S2^*$ have been expected to arise from Ga-Sb bonding.[17,32] The surface sensitivity of these "$S2$" components (Table I) supports this assignment. The Ga spectrum of Sb/GaAs(100)(2×4) and its fitting are consistent with the corresponding ones for the As/GaAs(100)(2×4) surface.[19,20]

Deconvolution of the Sb $4d$ spectrum from the (2×4) surface in Fig. 3 shows two components $S1^*$ and $S2^*$, which indicates two different chemical bonding environments for Sb atoms on the (2×4) surface, indicating the further presence of two different Sb bonding sites on this surface. It is worth noting that the fitting of this Sb spectrum by only the one doublet increased clearly the component width, whereas the addition of a third doublet led to no significant increase in quality of the fit, as one could expect if the third component was genuinely present. The intensity ratio $S1^*/S2^*$ equals nearly unity (Table I) proposing the same Sb occupation in both sites. This is perhaps the most striking point in the present core-level study that the Sb spectrum from the (2×4) surface reveals the two components, instead of one found previously.[17,32] This result is however in agreement with previous core-level studies of As/GaAs(100)(2×4) surface,[18–20] which indicate the presence of two surface-related contributions in As $3d$ for that surface. Moreover, the appearing of these Sb components $S1^*$ and $S2^*$ is consistent with our structural analysis of the (2×4) surface showing the δ_2 structure which includes two inequivalent Sb-dimer sites in the unit cell. We will return to the core levels below with structural models.

Figure 3 shows that three components $S1$, $S2$, and $S3$ were resolved from the Sb $4d$ spectrum of the (2×8) surface, indicating three different Sb bonding environments coexisting in this structure. This deconvolution is very similar to that found for the (2×8) surface in Ref. 32. Since the (2×8) surface is more group-V-rich than the (2×4) one, and no $S3$-like component is observed in the (2×4) spectrum, it is reasonable that $S3$ originates from Sb atoms in an elemental, Sb-bulklike structure (i.e., only Sb-Sb bonding).[29,32] Refering these previous investigations, we assign $S1$ in the (2×8) spectrum to Sb atoms that have bonded to Ga atoms (Sb-Ga). Note that Sb atoms with Sb-Ga can also be bonded to Sb atoms. $S2$ is also assigned to Sb-Ga in the next section where intensity ratios of the components are compared with a proposed (2×8) structural model.

B. STM experiments

As described in Sec. II, similar LEED patterns were observed from the Sb/GaAs(100)(2×4) and (2×8) surfaces in the both vacuum systems for the photoemission and STM measurements. Figures 4(a) and 4(b) show typical (2×4) and (2×8) LEED patterns, which were taken from the sample used in STM experiments. Next, we present STM results of the Sb/GaAs(100)(2×4) surface whereas the interpretation of STM images from the (2×8) reconstruction is more clear. Imaging the filled density of states, we observe dangling bonds of the group-V atoms, because in the $III-V$ reconstruction group-V bonds are filled and group-III dangling bonds empty on the basis of the electron counting model (ECM).[40] The filled-state STM image of the (2×4) surface shown in Fig. 5(a) is characterized by a series of dark and bright rows running along [0–11] direction with good long-range order and low kink density. A separation of the rows is ~16 Å indicating the ×4 periodicity. As can be seen

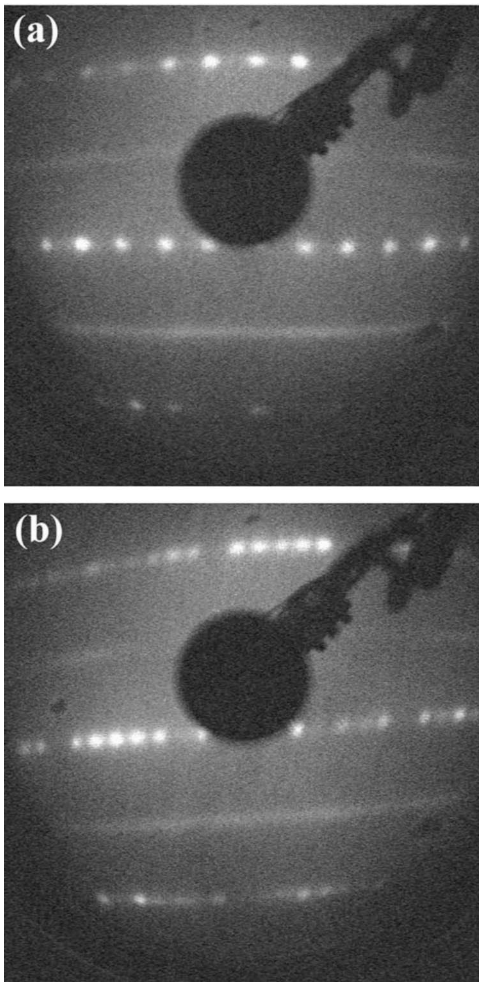

FIG. 4. Typical LEED patterns from the Sb/GaAs(100)(2×4) (a) and (2×8) (b) surfaces within STM experiments.

in a high-magnification filled-state image [Fig. 5(c)], the rows are composed of bright protrusions, slightly oval in shape, which are oriented along the rows with a separation of ~8 Å in the [0–11] direction, arranging the 2× periodicity on this surface. The 2× periodicity (dimerization) in the [0–11] direction can be confirmed by a line profile along the bright rows, which is similar to that presented later in Fig. 6(d) for the (2×8) reconstruction. A typical line profile along the [011] direction in Fig. 5(e) differs from those shown for the GaAs(100)(2×4)β2 and α phases,[12] of which the two top dimers can be resolved as two symmetric peaks in profiles. Such a double-peak profile has been found only very rarely in our analysis. This strongly proposes that the (2×4) structure, which contains one dimer in the top layer per unit cell (i.e., δ-type structure), dominates clearly. Also, the bright protrusions in Fig. 5(c) are slender along the [011] direction as compared to those of the GaAs(100)(2×4) phases in Ref. 12, supporting the one top-dimer structure. There seem to be two (2×4) unit cells due to a top-dimer displacement of ~4 Å in the [011] direction. However, we rarely observe extended "zigzag" single-dimer rows, that is, some correlation between unit cells in the [0–11] direction can be expected.[23] Figure 5(c) suggests that the dark rows, i.e., the bottom of the missing top-dimer trenches, exhibit their own structure seen as faint gray features in the center of the dark rows, in the filled-state mode. A line profile of this faint structure along the dark rows, which is very similar to that in Fig. 6(d), shows the 2× periodicity in the [0–11] direction. Thus, we propose that the dark rows are also composed of the group-*V* dimers whose axis is aligned in the [0–11] direction. We also note that the depth in the orthogonal profile in Fig. 5(e) is consistent with the depth found for the structure having a dimer in the third layer.[11,12] Both the top and bottom dimers are assigned here to the Sb dimer. We rule out the presence of As dimers on the Sb/GaAs(100)(2×4) because the photoemission measurements showed only the GaAs bulklike, fourfold coordination for As atoms in this structure. A depth profile analysis shows a vertical distance, measured from the bottom of the trench to the top Sb dimer, to be 1.5–1.8 Å in the filled-state mode. As this distance is slightly larger than a depth of 1.4 Å measured for the GaAs(100)(2×4)β2 phase,[12] our observation is in agreement with previous studies,[21–23,26] which show an upward movement of the single top dimer.

Figure 5(b) shows the dual-polarity STM image where a black arrow indicates the tip position when a sample bias was reversed from the filled to an empty-state mode. That is, the upper and lower parts of this image are the unoccupied and occupied orbital STM images, respectively. Imaging the unoccupied density of states, we observe dangling bonds of Ga atoms.[40] Therefore, the bright rows of the empty-state images [Figs. 5(b) and 5(d)] correspond to Ga atoms, and we conclude that the (2×4) surface includes Ga atoms. This is well consistent with previous studies of Esser *et al.*[25] who have found Ga dimers on the Sb/GaAs(100)(2×4) surface by RAS measurements. Figure 5(b) presents that the bright and dark rows observed in the empty-state mode are quite well aligned with the rows of the filled-state image, which can be understood with the structure where Ga atoms are located on the surface between the top and bottom layer Sb-dimer chains. The magnified empty-state image in Fig. 5(d) proposes that Ga atoms form dimers observed as bright cigar-shaped protrusions oriented along the [011] direction, i.e., perpendicular to the Sb-dimer-bond direction. The separation of these protrusions is ~4 Å in the [0–11] direction, that is, the (2×4) unit cell includes two Ga dimers. An analysis of the line profiles for the empty-state images along the [011] direction (i.e., the Ga dimer bond direction) does not present a Ga dimer as a double peak in the profile. As can be seen in Fig. 5(f), which shows a profile in the empty-state mode, only one peak rather than the double-peak contour within resolution is observed, which is most likely due to a short Ga dimer-bond length. In fact, a very short bond length of 2.45 Å has been found for Ga dimers.[25,26]

Comparing our observations with earlier-reported STM studies of the Sb/GaAs(100)(2×4) structure,[23,24] we find close similarities between filled-state images of this study and those shown by Moriarty *et al.*[23] who have proposed the δ_1 model. Recently, Whitman *et al.*[24] have reported a new (2×4) structure of which unit cell contains two Sb dimers and one As dimer in the first, top layer. To prepare the (2×4) reconstruction, they used a much lower temperature

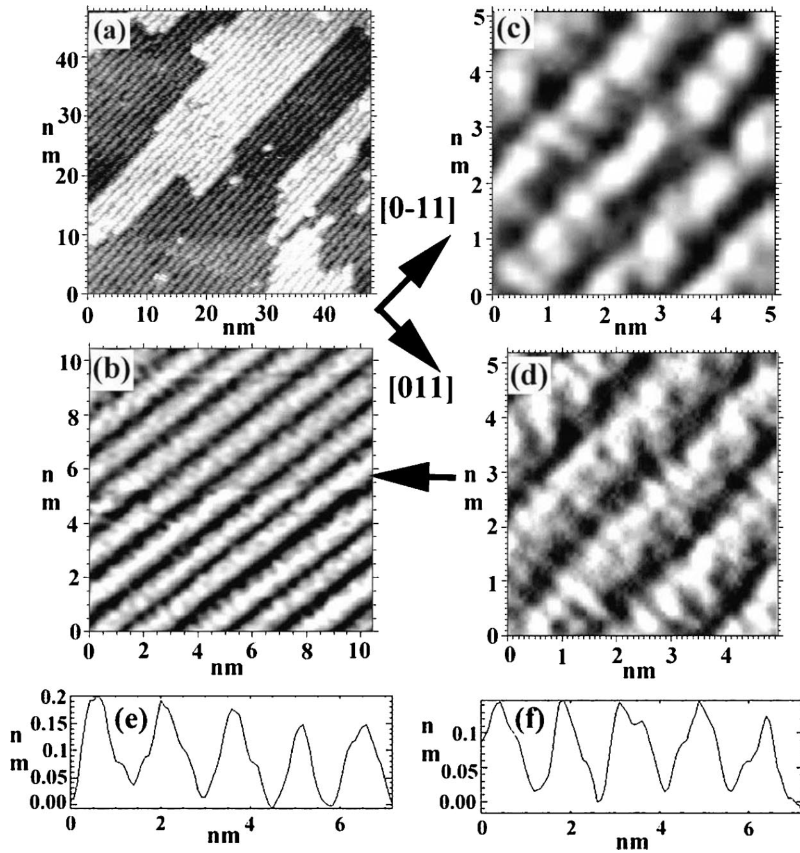

FIG. 5. STM images and line profiles of the Sb/GaAs(100)(2×4) surface. (a) Filled-state image: $48\times48\ \mathrm{nm}^2$, 2.7 V, 95 pA. (b) Reversed-bias image with the bias change from the filled-state (the bottom part of the image) to the empty-state mode (the top part) during scanning: $10.5\times10.5\ \mathrm{nm}^2$, 2.7 V, 91 pA. (c) High-magnification filled-state image: $5.0\times5.0\ \mathrm{nm}^2$, 2.7 V, 95 pA. (d) High-magnification empty-state image: $5.0\times5.1\ \mathrm{nm}^2$, 2.7 V, 91 pA. (e) Typical line profile in the filled-state mode along the [011] direction. (f) Line profile in the empty-state mode along the [011] direction.

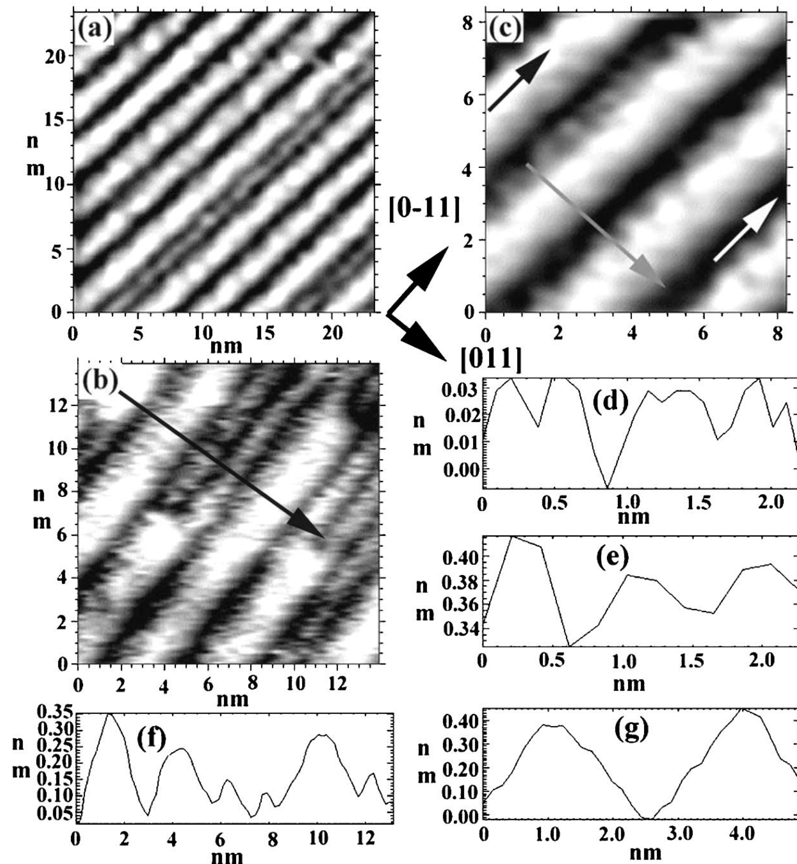

FIG. 6. Filled-state STM images and line profiles of the Sb/GaAs(100)(2×8) surface. (a) $23\times23\ \mathrm{nm}^2$, 2.6 V, 100 pA. (b) The image of the intermediate surface between the (2×4) and (2×8) reconstruction (see the text): $14\times14\ \mathrm{nm}^2$, 3.2 V, 91 pA. (c) High-magnification image: $8.5\times8.5\ \mathrm{nm}^2$, 3.0 V, 200 pA. (d) Line profile along the white arrow in (c). (e) Profile along the black arrow in (c). (f) Profile along the black arrow in (b). (g) Profile along the gray arrow in (c).

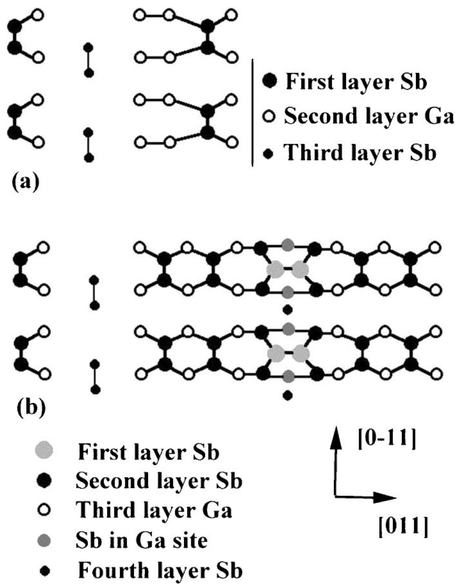

FIG. 7. Structural models for Sb/GaAs(100)$(2\times4)\delta_2$ (a) and (2×8) (b). Note that the fourth-layer Sb atoms in the center of the (2×8) row just below the top dimer have not been marked in the (2×8) model for clarity.

(460 °C) for heating the Sb-induced GaAs(100)(2×8) surface compared to that in present work (550 °C). In fact, such a difference in the temperature can cause drastic changes in structure and stoichiometry. In conjunction with the core-level analysis, our STM observations and line-profile data together show the δ_2 structural model for the Sb/GaAs(100)(2×4) surface [Fig. 7(a)], giving support to generality of the $III-V(100)(2\times4)\delta$ model. The found δ_2 structure is also consistent with valence-band results in Sec. III C. Furthermore, we emphasize that this δ_2 model shows two inequivalent Sb surface sites, i.e., the top and third-layer Sb dimers. This is in agreement with the Sb core level from the (2×4) surface revealing the two components $S1^*$ and $S2^*$. Moreover, the δ_2 model shows the same number of Sb atoms occupying these two inequivalent bonding sites on this surface, and on the other hand, the Sb $4d$ spectrum presents the almost equal intensities for the $S1^*$ and $S2^*$ components. Therefore, we connect these components $S1^*$ and $S2^*$, which are results of different environments for Sb, to the two inequivalent dimer sites. The result agrees with previous studies of As/GaAs(100)(2×4) surface,[18–20] which indicate the presence of two dimer-related contributions in As $3d$ for that surface, and further can provide useful data for characterizing of the $III-V$ surfaces with the similar geometry. Because of the upward movement of the top Sb dimer, it is more isolated than the third-layer one, and tentatively, the screening of the core hole in the photoemission is reduced for the top dimer, as compared to the third-layer one. Thus, we assign the higher BE-side component $S2^*$ to the top Sb dimer of the δ_2 model and the $S1^*$ component to the third-layer one.

Furthermore, we propose that the Ga component $S2^*$ of the (2×4) spectra, which was assigned to Ga atoms bonded to Sb,[17,32] arises from the second-layer Ga atoms of the δ_2 structure rather than the fourth-layer Ga atoms bonded to the Sb dimers because the fourth-layer ones are fourfold-coordinated and basically have a similar environment to the bulk component. (We note that the bulk binding energy of Ga $3d$ is 0.1 eV higher for GaSb than GaAs.[35]) The δ_2 model shows that there are, in fact, three inequivalent Ga sites in the second layer, i.e., threefold-coordinated Ga bonded to Sb, fourfold-coordinated Ga-dimer atom bonded to Sb, and a threefold-coordinated Ga-dimer atom. Therefore, we tentatively connect the lower BE Ga component $S1^*$ also to the one or two inequivalent second-layer Ga atoms.

Figure 6(a) shows a filled-state STM image of the Sb/GaAs(100)(2×8) surface. The surface is characterized by a series of dark and bright rows which run along the [0–11] direction and alternate in the [011] direction with a separation of ~32 Å, arranging the $\times8$ periodicity. As seen in Fig. 6(a), this $\times8$ ordering is occasionally interrupted due to a faint narrow row between the main rows. A lateral distance of this faint row measured from the bright one is 20 or 24 Å. Before the depth profile analysis and closer structural examination of the (2×8) reconstruction, we consider initial stages of the formation of the (2×8) surface. Figure 6(b) shows a typical filled-state image from a separate Sb-induced surface which was prepared as the (2×8) sample described in Sec. II (Sample C), but the evaporation time of Sb was shorter (~15 min). This separate surface can be tentatively assumed to present an intermediate phase involved in the transition between the Sb/GaAs(100)(2×4) and (2×8) reconstructions. As seen from Fig. 6(b), the surface is a mixture of the (2×4) and (2×8) domains. Figure 6(b) and a depth profile in Fig. 6(f) reveal the presence of two different top structures of the (2×8) row with the vertical distance of about 2.1 and 3.5 Å measured from the bottom of the dark row. This can result from the fact that the top Sb dimer is missing on the lower (2×8) row, as realized later with our structural model. Likewise, the top of the lower (2×8) rows located at a higher height level than the (2×4) one, which can be explained by the Sb antisite (Sb_{Ga}) formation in the region of the (2×4) trench when "pairing" of the (2×4) rows occurs and the missing 0.25-ML Ga row is filled in during the Sb evaporation.[24]

Figure 6(c) shows a magnified filled-state image of the (2×8) surface where white, black, and gray arrows represent positions of the line profiles shown in (d), (e), and (g), respectively. The profile of the dark row in Fig. 6(d) shows a dimer-like structure with the $2\times$ periodicity similar to that observed for the $(2\times4)\delta_2$ trenches. Therefore, we propose that the dark rows are composed of dimers. The gray chain features running along the [0–11] direction between the white and black ones also exhibit the similar $2\times$ periodicity (not shown). Furthermore, the depth profile along the black arrow in Fig. 6(e) reveals the $2\times$ structure for the center of the top row. In contrast, the single-peak rather than double-peak contour of the top row indicates the orthogonal dimer-bond direction compared to the dimer orientation in the dark and gray rows. Figure 6(c) shows a two-step structure for the (2×8) rows which are composed of the white and gray chain features running along the [0–11] direction in the image with the characteristic height of 3.5 and 2.1 Å measured

from the dark row, respectively. Our analysis of STM images suggests the structure, where the white top row is symmetrically centered between two gray ones, to dominate.

Only a structural model has been presented so far for the Sb/GaAs(100)(2×8) surface.[24] Our measurements are not fully consistent with this model. A significant difference is observed in the dark row structure: the present analysis shows the dimer structure for the bottom of the trenches in contrast to that in Ref. 24. We propose in Fig. 7(b) a new, modified structural model for Sb/GaAs(100)(2×8) which obeys ECM, contrary to the previous one. In this new model, Sb dimers form in the three atomic layers. The (2×8) unit cell consists of one top-layer Sb dimer, which is oriented along the [011] direction on the center of the row, four second-layer Sb dimers oriented in the [0–11] direction, and one Sb dimer sitting in the fourth layer with the dimer bond also along the rows. As discussed above with Figs. 6(b) and 6(f), when the area of the unit cell increases by two times, i.e., the (2×8) unit cell spans the two $(2\times4)\delta_2$ units, the most likely candidate for filling in the missing Ga row is Sb_{Ga}. The Sb antisites serve four extra electrons per unit cell, but the two second-layer Sb atoms, which are bonded to the top dimer, need two electrons more than Sb dimer in this structure. Furthermore, our model shows that there are Sb atoms in the four atomic layers in the center of the row, and the total Sb coverage of Sb/GaAs(100)(2×8) is 1.25 ML. However, the amount of Sb can be less if As atoms are involved in the (2×8) surface structure, as the deconvolution of As $3d$ proposed in Sec. III A. In this case, the substitution of Sb by As atom occurs most likely,[24] and this replacement of Sb lowers the Sb coverage. (As atoms are not shown in the model for simplicity.) The presence of the higher binding-energy As component $S2$ (Fig. 1), which was less surface sensitive, and was associated with the group-V–group-V bonding, can agree with the structure where the As atom replaces the buried Sb atom bonded to Sb in the center of the row.

The proposed model shows that Sb/GaAs(100)(2×8) is locally, in the middle of the row, identical to chainlike structures of the GaSb(100)(2×10) and $c(2\times10)$ surfaces,[30,31] as found in Ref. 24. Also, according to our measurements as well as previous results,[24,32] the Sb/GaAs(100) system forms no $c(4\times4)$ structure, similarly to the Sb/GaSb system. The found similarities suggest that some characteristics of the interaction between the Sb layer and the GaSb(100) surface can apply also for the Sb/GaAs(100) system in the monolayer regime. Whitman *et al.*[30,31] have shown that GaSb forms the (2×10) and $c(2\times10)$ structures instead of the $c(4\times4)$ one, common to many III-As and III-Sb compounds, because of the excellent lattice match between GaSb(100) and the elemental Sb combined with a low stiffness of GaSb. The bulk-terminated GaAs(100) unit cell (4.0 Å) is smaller than the GaSb one (4.3 Å) and, therefore, clearly less matched to the elemental Sb (4.3 Å).[31] That is, the GaAs lattice imposes the lateral distance constraint of 4.0 Å for the second-layer (and lower) Sb atoms in the middle of the (2×8) row. Perhaps more importantly, as they pointed out, the Ga-Sb bond is one of the softest of the $III-V$ compounds, decreasing the strain energy and balancing the Sb-dimer-mediated stress (see Ref. 30 and reference therein). In contrast, on the $III-V(100)c(4\times4)$ surfaces, such as As/GaAs(100)$c(4\times4)$, this dimer-mediated stress is proposed to be relieved through the periodic arrangement of dimer vacancies. Thus, referring these previous investigations, we propose that the net effect is the stable Sb/GaAs(100)(2×8) surface with the continuous Sb-dimer rows. Note that the proposed (2×8) model, in which more Sb atoms are bonded to Ga than purely to Sb atoms, is consistent with a key role of the softness of Ga-Sb in the formation of the chainlike (2×8) surface instead of the $c(4\times4)$ one.

Finally, we compare more the structural model with the core-level results. The Ga $3d$ component $S2$ was assigned, as $S2^*$ of the (2×4) surface, to the Ga atoms that have bonded to Sb. According to the proposed model in Fig. 7, the (2×8) unit cell includes the threefold-coordinated Ga atoms bonding to Sb in the row edge, which are inequivalent to the fourfold-coordinated Ga-Sb sites and might result in $S2$. We speculate that due to the local Sb-Sb bulklike structure in the row center, the environment for the fourfold-coordinated Ga atoms can vary. That is, two or more different Ga-Sb bonding sites, which produce the both Ga components $S1$ and $S2$, can appear in the (2×8) unit cell. The $S1$ is relatively less surface sensitive (Table I) suggesting its origin reside in the subsurface, as compared to $S2$. The fitting of the Sb $4d$ spectrum from the (2×8) surface revealed the three dominant components $S1$, $S2$, and $S3$ indicating three different chemical environments for Sb atoms in the structure. The lowest BE component $S1$ was assigned to the Sb-Ga bonding and the highest BE component $S3$ to Sb atoms in the elemental structure (Sb-Sb), that have not bonded to Ga atoms. These assignments are tentatively consistent with the proposed (2×8) model which includes such Sb atoms. In fact, the model proposes six inequivalent Sb sites per unit cell: (1) second- and fourth-layer Sb-dimer atom bonded to a fourfold-coordinated Ga, (2) row-edge dimer atom in the second layer bonded to threefold-coordinated Ga, (3) second-layer atom bonded to the top dimer, (4) top dimer site, (5) Sb_{Ga}, and (6) buried fourth-layer Sb, of which the occupation proportion is 3:2:2:1:1:1, respectively. The present results do not allow us to consider the further possible origins of the core components among those Sb sites. However, to clarify whether $S2$ is related to Sb atoms bonding to Ga atoms (i.e., Sb-Ga) or not, we consider the ratio of the number of the elemental Sb-Sb atoms divided by the amount of Sb atoms bonded to Ga for Sb/GaAs(100)(2×8). According to the (2×8) model, this ratio of the number of Sb atoms, which have not bonded to Ga, to the number of Sb atoms, which bond to Ga atoms, is 0.25. Note that the above sites 1, 2, 3, and 6 correspond Sb-Ga, and the sites 4 and 5 correspond Sb-Sb. On the other hand, if the $S2$ is due to the Sb-Ga bonding like $S1$, the intensity of the component $S3$ divided by the combined intensity $S1+S2$ equals 0.46 at the 60°-emission and 0.29 at the normal emission. In contrast, if $S2$ is assigned, similarly to $S3$, to Sb atoms which have not bonded to Ga, the intensity ratio of $S2+S3$ to $S1$ equals 1.86 at the 60°-emission and 1.36 at the

normal emission. Although all the photoelectron attenuation and diffraction effects have been ignored in the core-level data, and despite the fact that the replacement of Sb by As atoms at the surface can change the ratio, the above comparison clearly proposes that $S2$ is related to Sb atoms that have bonded to Ga, disagreeing with the previous core-level analysis.[32]

C. Photoemission from valence-band region

Valence-band photoemission spectra have been measured from the Sb/GaAs(100)(2×4) and (2×8) surfaces as a function of the polar angle θ_p along the [0–11] and [011] azimuths, corresponding to the surface parallel wave vector $\mathbf{k}_\parallel$ lying on the symmetry lines between the symmetry points Γ and J' and between the points Γ and J in the surface Brillouin zone (SBZ), respectively. We have utilized the symmetry point notation of Larsen *et al.*[28] to indicate the SBZ of the symmetry point by a subscript (e.g., $J'_{(1\times1)}$, $J'_{(2\times4)}$). The parallel wave vector $\mathbf{k}_\parallel$ is related to the electron kinetic energy E_k and emission angle θ_p by the expression

$$k_\parallel=\left(\frac{2m}{\hbar^2}E_k\right)^{1/2}\sin\theta_p\,. \tag{1}$$

Experimental angular and energy resolutions cause an uncertainty in $\mathbf{k}_\parallel$ because

$$\Delta k_\parallel=\left(\frac{2m}{\hbar^2}E_k\right)^{1/2}\left(\frac{\sin\theta_p}{2E_k}\Delta E_k+\cos\theta_p\Delta\theta_p\right). \tag{2}$$

If the maximum experimental inaccuracy is expected, $\Delta E=0.3$ eV and $\Delta\theta=2°$, then $\Delta k_\parallel=0.07$ Å^{-1} for a typical kinetic energy of 15 eV at near normal emission. This resolution can hinder realizing the bands along the ΓJ direction, i.e., the $\times4$ $(\times8)$ ordering direction, implying a fourfold (eightfold) periodicity.

The valence spectra were corrected for a smooth background by a standard 30-point adjacent averaging procedure and they were aligned to the VBM. Also, the weak emission features near the energies of the GaAs bulk critical points X_3 and $\Sigma_1^{\min}$ at binding energies of 6.7 and 4.0 eV,[41,42] respectively, provided an additional check for the valence-band alignment. Figure 8 shows the valence spectra of the Sb/GaAs(100)(2×4) surface and the peak positions for a number of polar angles along the [0–11] azimuth. Two bulk valence-band features (i.e., primary-cone peaks), $B1$ and $B2$ at near binding energies of 1 and 3 eV have been identified with previous studies of GaAs electronic structure.[41,42] We find that $B1$ and $B2$ disperse to the higher BE between the Γ and $J'_{(1\times1)}$ points, in consistency with previous ARPES measurements of different $III-V(100)(2\times4)$ surfaces.[28,43,44] Apart from the bulk contributions, two spectral features $S1$ and $S2$, which can be surface related, are observed at the lower BE than the bulk ones. The $S2$ feature is more pronounced with an initial energy dispersion of 0.4 eV. For $S2$, a maximum BE of 1.0 eV is near the normal emission (Γ point), and a minimum BE of 0.6 eV is close to $\theta_p=12°$ ($J'_{(2\times4)}$ point). The $S2$ band dispersion (i.e., energy versus $k_\parallel$ plot) presented later in Fig. 12 shows the twofold periodicity in the [0–11] direction. In contrast, the $S1$ feature at ~0.4 eV, which appears as a shoulder of $S2$, does not disperse clearly with the momentum.

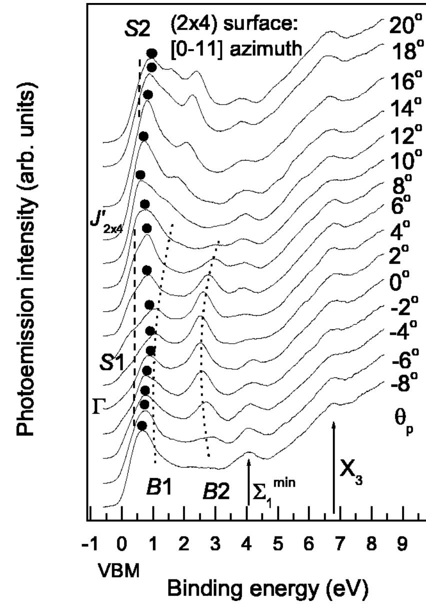

FIG. 8. Photoemission spectra as a function of polar angle for the Sb/GaAs(100)(2×4) surface in the [0–11] azimuth.

Figure 9 shows the spectra from the (2×4) surface along the [011] azimuth corresponding $\mathbf{k}_\parallel$ lying on the ΓJ symmetry line. The $B1$ and $B2$ bands show the similar BE and dispersions along this orthogonal azimuth. The similar features $S1$ and $S2$ also appear. However, the $S2$ feature is not as prominent as it was in the azimuth [0–11]. This can indicate that $S2$ consists of some character of p_x symmetry, corresponding the [0–11] azimuth, because the intensity of states, which show some p_{xy} symmetry, can change with the

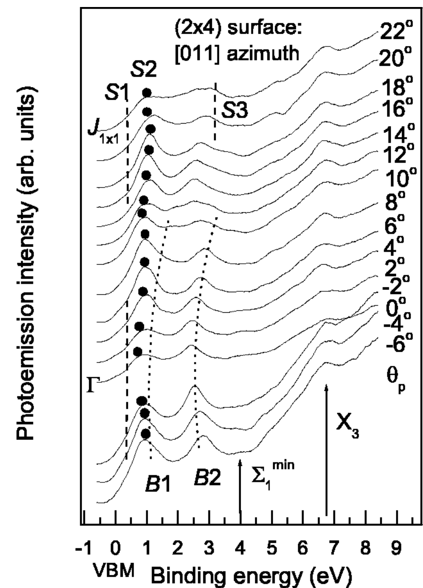

FIG. 9. Photoemission spectra as a function of polar angle for the Sb/GaAs(100)(2×4) surface in the [011] azimuth.

azimuthal angle of the incident electric field, while the p_z intensity (p_z corresponds to symmetry normal to the surface) remains constant at the fixed angle of incidence. Also, the energy dispersion of $S2$ is lower, which can be expected because of the small SBZ size in this $\times 4$ direction. We propose however a weak fourfold periodicity of the (2×4) SBZ for the $S2$ band in the [011] direction (Fig. 12). In the [011] direction, a new state labeled $S3$ is proposed around the $J_{(1\times 1)}$ point at BE near 3 eV.

Next we examine whether the spectral features $S1$ and $S2$, which were not identified as bulk excitations, are surface derived. $S3$ is assigned later within a comparison to band-structure studies of As/GaAs(100)(2×4). $S1$ and $S2$ do not reveal the most direct surface-state criteria, namely, that a state, which is located in a gap of the bulk-band projection into the reduced SBZ, can be identified as a surface state. Thus, $S1$ and $S2$ can be surface resonance coupling to bulk states at the same energy by the surface umklapp process through reciprocal lattice vectors of the (2×4) reconstruction. The clear $2\times$ surface periodicity of the band $S2$ proposes that it is a real surface state. Likewise, the surface-structure dependence of $S1$ and $S2$ [i.e., the (2×4) versus (2×8) surface], as seen later, supports their surface-state character. Also, the features $S1$ and $S2$ are consistent with theory. Schmidt and Bechstedt have performed electronic-structure calculations for the Sb/GaAs(100)$(2\times 4)\beta 2$, δ_1, and δ_2 surfaces.[26] Their calculations show surface states in the range of 0.2–0.7 eV below VBM for the Sb/GaAs(100) $\times(2\times 4)$ structures. The band structures of these three (2×4) phases are quite similar due to the same reconstruction elements.[26] Schmidt and Bechstedt have shown the two highest occupied states of the δ_2 structure at 0.23 and 0.33 eV below VBM at K point to be related to antibonding and bonding combination of p_z orbitals localized at the third-layer Sb dimer, respectively, and furthermore that the two higher BE states at $\sim$0.4 eV correspond to dangling p_z orbitals localized at the top dimers.[26] Their calculations also show a weakly localized state at $\sim$0.6 eV which corresponds to a bonding state of the top Sb dimer (Fig. 12, later). Because here the energy dispersions have not been mapped along the $J'K$ and JK directions, the measurements cannot be compared carefully between the calculated dispersions of the $\beta 2$, δ_1, and δ_2 surfaces. However, the characters (i.e., the energy position and relative dispersion strength) of features $S1$ and $S2$ are consistent with the calculated states of the δ_2 structure. We note in passing that two highest states of As/GaAs(100)(2×4) surface, which $S1$ and $S2$ resemble closely as seen below, disperse only slightly along the JK line, and their energy positions are almost identical in the J and K points.[28] To summarize, $S1$ and $S2$ are assigned as Sb-induced surface states. On the basis of these previous calculations, the more dispersive feature $S2$ is connected to the weakly localized top-Sb-dimer state, and the $S1$ arises most likely from dangling bonds of the top- and/or third-layer dimers of Sb/GaAs(100)$(2\times 4)\delta_2$.

It is also instructive to compare our measurements with previous electronic-structure results of the As/GaAs(100)(2×4) surface by Larsen *et al.*[28] (Fig. 12, later). The BE of the states $S1$ and $S2$ are almost identical to BE of two highest states of As/GaAs(100)(2×4) surface found in Ref. 28, where these states have been shown to be As dangling-bond-related sp_z-like surface states. This is well consistent with theory presenting this BE equaling, which is shown to be due to the different As- and Sb-dimer lengths.[26] The As dangling-bond states have been shown to own some p_x symmetry.[28] We also suggested some p_x symmetry for the $S2$ state. The feature $S3$ around the $J_{(1\times 1)}$ point at $\sim$3 eV resembles a surface state found by Larsen *et al.* who have shown this state, which is also found at a BE of $\sim$3 eV, to be related to the As dimer bond. Calculations of Schmidt and Bechstedt have shown that this As-dimer state can be related to the σ-type bond which arises from σ and π combinations of the dehybridized As dangling bonds,[45] but such higher BE states have not been mapped in their calculations of the Sb/GaAs(100)(2×4) surface.[26] However, referring to these previous As/GaAs(100)(2×4) studies, we tentatively relate the $S3$ feature to Sb dimers. We would like to emphasize that we observe slightly stronger dispersion for the $S1$ and $S2$ states of Sb/GaAs(100)(2×4) than that found in Ref. 28 for the As-induced states. That can be seen in the $S2$ dispersion in the [0–11] direction, where the twofold periodicity is found for both systems. The bandwidth of the $S2$ state is 0.4 eV, while the bandwidth of 0.3 eV has been found for the similar state of the As/GaAs(100)(2×4) surface in the [0–11] azimuth. Such an increase in the bandwidth can indicate a somewhat stronger interaction between the bonds in the Sb/GaAs(100)(2×4) system, as compared to As/GaAs(100)(2×4). This is consistent with the idea that the geometry is the same for the both systems but the adsorbate size is different. That is, the covalent radii of Sb (1.38 Å) is larger than that for As (1.19 Å), and therefore the wave-function overlap in the Sb-dimer rows can increase (see Ref. 8 and references therein). To recapitulate, the observed similarities for the band structures of the Sb and As/GaAs(100)(2×4) surfaces support that the similar model can be used to describe these two systems.

For the Sb/GaAs(100)(2×8) surface, we find the bulk emissions $B1$ and $B2$ with the same BE and dispersion as for the (2×4) one (Figs. 10 and 11). The bulk critical-point contributions are also found in the spectra, providing an additional check for the valence-band alignment. In general, some broadening of the features is observed in the (2×8) spectra, as compared to the (2×4) ones, which can be due to the umklapp processes associated with the short surface reciprocal lattice vectors of the (2×8) structure or that the (2×8) surface is less ordered than the (2×4) one. Furthermore, several surface states within a small BE separation might contribute in the broadened feature near VBM. Apart from the bulk contributions, three weakly dispersive surface-related features labeled $S1^*$, $S2^*$, and $S3^*$ are proposed in Figs. 10 and 11. The feature $S1^*$ at $\sim$0.5 eV is relatively more pronounced than $S1$ in the (2×4) spectra. Also, we find that $S1^*$ is slightly more prominent in the [011] azimuth than the [0–11] one which proposes, as described above, that $S1^*$ contains some characteristics of p_y orbitals, corresponding to the [011] direction. Such a polarization dependence

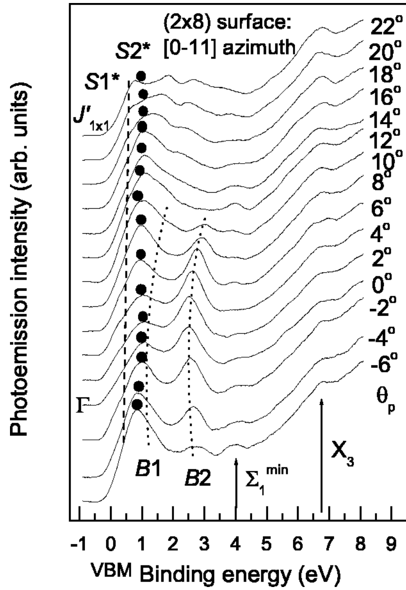

FIG. 10. Photoemission spectra as a function of polar angle for the Sb/GaAs(100)(2×8) surface in the [0–11] azimuth.

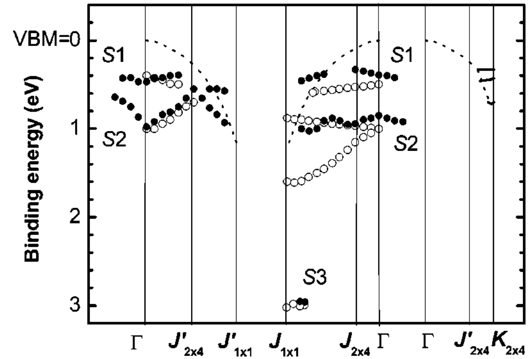

FIG. 12. Energy dispersions of the surface-related states (solid symbols) mapped for the Sb/GaAs(100)(2×4) surface in the [0–11] and [011] azimuths, corresponding to the $\Gamma J'$ and ΓJ symmetry directions of SBZ. The bands of the As/GaAs(100)(2×4) surface are indicated by open symbols (from Ref. 28). Dashed lines show edge of the projected bulk-band structure of GaAs, and thick solid lines show calculated states of Sb/GaAs(100)(2×4)δ_2 (from Ref. 26).

was not observed for the $S1$ state. Thus, we relate the $S1^*$ feature to a new surface-derived state. We remark that two or more overlapping states might contribute in the $S1^*$ feature. To get insight into the possible structural origin of the $S1^*$ state, which was not observed for the (2×4) surface, we resort to the qualitative comparison with the model. The determined model shows that in addition to the Sb dimers oriented in the [0–11] direction, the Sb/GaAs(100)(2×8) surface includes also Sb dimers which are oriented in the orthogonal [011] azimuth in the top layer. In analogy with that the dimers oriented in the [0–11] direction show some p_x symmetry,[28] such bond of top-dimer along the [011] direction can own some p_y symmetry, and thus we propose that the new $S1^*$ state arises from bond of the top Sb dimer. The $S1^*$ dispersion is weak which indicates a weak interaction and further may be an indication of localized bonds.

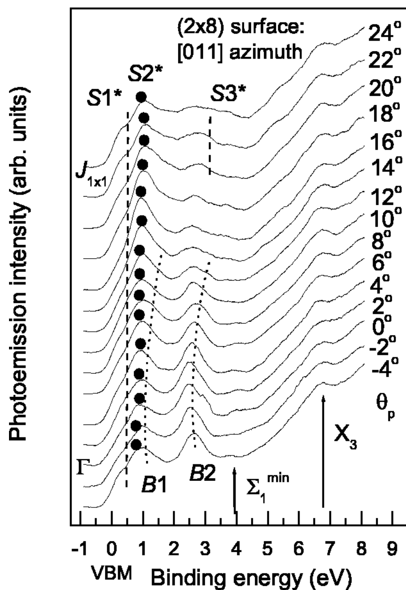

FIG. 11. Photoemission spectra as a function of polar angle for the Sb/GaAs(100)(2×8) surface in the [011] azimuth.

We assign the $S2^*$ feature, which resembles the $S2$ of the (2×4) spectra, to the second- and/or fourth-layer Sb dimers with the bond direction of [0–11] because the $S2^*$ band dispersion is reminiscence of a weak twofold periodicity of the (2×8) SBZ in the [0–11] azimuth. The $S3^*$ state, which is observed at near the $J_{(1\times1)}$ point at BE of ~3 eV as in the (2×4) spectrum, is similarly connected to Sb dimers. It is worth pointing out that the $S3$-like dimer-bond state does not appear in the structure of As/GaAs(100)$c(4\times4)$ due to the trigonal bonding of the As dimer (i.e., the As dimers are bonded to the underlying As layer).[38] This proposes the (2×8) structure to include similar Sb dimers to those of the δ_2 surface, which bond to Ga, in consistency with the proposed (2×8) structural model. Finally we observe that no considerable emission appears above VBM for the (2×4) and (2×8) surfaces indicating their semiconducting character, in good agreement with the structural models which both obey ECM.

IV. SUMMARY

We have studied the electronic, geometric, and chemical properties of the Sb/GaAs(100)(2×4) and (2×8) surfaces by means of core-level and valence-band photoemission and STM measurements. Combining these results and showing good consistency among them, we have verified that the Sb/GaAs(100)(2×4) surface is well compatible with the δ_2 model. This result supports generality of the δ-type model among the $III-V$(100)(2×4) surfaces. Deconvolution of the Sb $4d$ spectrum from the (2×4) surface shows two components with the energy difference of 0.44 eV. We connect tentatively these two Sb components to two inequivalent Sb dimers of the δ_2 unit cell. ARPES measurements from the Sb/GaAs(100)(2×4) surface along the $\Gamma J'$ and ΓJ symmetry lines show the surface-derived states $S1$ and $S2$ at ~0.4

and ~0.6 eV below VBM, respectively, which have been identified with previous electronic-structure calculations of the same surface.[26] The more dispersive feature $S2$ is connected to the weakly localized top-Sb-dimer state, and the $S1$ arises most likely from dangling bonds of the top- and/or third-layer dimers of Sb/GaAs(100)$(2\times4)\,\delta_2$. The comparison of the valence-band results with previous measurements of the As/GaAs(100)(2×4) surface[28] reveals that the $S1$ and $S2$ states locate nearly the same BE as the highest surface states of As/GaAs(100)(2×4). Several similarities found for the band structures of the Sb/GaAs(100)(2×4) surface and the As-stabilized one support that the similar model can be used to describe these two systems.

For the Sb/GaAs(100)(2×8) surface, we propose a new structural model with the Sb coverage of 1.25 ML, which obeys the electron counting model and consists of Sb dimers in three atomic layers. The Sb $4d$ core-level spectrum of Sb/GaAs(100)(2×8) presents the three components. Two of these components have been assigned to Sb atoms with Sb-Ga and one component to Sb bonded only to Sb atoms (Sb-Sb). In analogy with the Sb/GaSb(100) system, the softness of the Sb-Ga bond is proposed to be a dominant reason why the Sb/GaAs(100)(2×8) surface is formed instead of the $c(4\times4)$ one. A new Sb-induced surface-derived state near 0.5 eV has been found in ARPES measurements of the (2×8) surface. This state has been qualitatively related to bond of the top-dimer chains on the underlying Sb layer.

ACKNOWLEDGMENTS

We thank Professor Q.-K Xue for discussions. We thank Mr. H. Ollila for technical assistance and gratefully acknowledge the MAX-lab staff. One of us (P. L.) would like to acknowledge financial support by the Graduate School of Materials Research (GSMR), and three of us would like to acknowledge financial support by the EC Access to the Research Infrastructure Program (ARI).

*Corresponding author. Electronic mail: pekka.laukkanen@utu.fi; fax: +358 2 333 6254.

[1] P. Skeath, C. Y. Su, W. A. Harrison, I. Lindau, and W. E. Spicer, Phys. Rev. B **27**, 6246 (1983).
[2] B. Z. Nosho, W. H. Weinberg, W. Barvosa-Carter, B. R. Bennett, B. V. Shanabrook, and L. J. Whitman, Appl. Phys. Lett. **74**, 1704 (1999).
[3] R. Ludeke, Phys. Rev. Lett. **39**, 1042 (1977).
[4] C. B. Duke, A. Paton, W. K. Ford, A. Kahn, and J. Carelli, Phys. Rev. B **26**, 803 (1982).
[5] P. Mårtensson, G. V. Hansson, M. Lähdeniemi, K. O. Magnusson, S. Wiklund, and J. M. Nicholls, Phys. Rev. B **33**, 7399 (1986).
[6] P. Mårtensson and R. M. Feenstra, Phys. Rev. B **39**, 7744 (1989).
[7] A. B. McLean, R. M. Feenstra, A. Taleb-Ibrahimi, and R. Ludeke, Phys. Rev. B **39**, 12925 (1989).
[8] D. N. McIlroy, D. Heskett, D. M. Swanston, A. B. McLean, R. Ludeke, H. Munekata, M. Prietsch, and N. J. DiNardo, Phys. Rev. B **47**, 3751 (1993).
[9] Z. Q. He, Y. O. Khazmi, J. Kanski, L. Ilver, P. O. Nilsson, and U. O. Karlsson, Phys. Rev. B **52**, 16602 (1995).
[10] H. Oscarsson, Z. Q. He, L. Ilver, J. Kanski, S. Mankefors, P. O. Nilsson, and U. O. Karlsson, Phys. Rev. B **61**, 2065 (2000).
[11] Q.-K. Xue, T. Hashizume, and T. Sakurai, Prog. Surf. Sci. **56**, 1 (1997).
[12] T. Hashizume, Q.-K. Xue, A. Ichimiya, and T. Sakurai, Phys. Rev. B **51**, 4200 (1995).
[13] A. Ohtake, J. Nakamura, S. Tsukamoto, N. Koguchi, and A. Natori, Phys. Rev. Lett. **89**, 206102 (2002), and references therein.
[14] N. Esser, W. G. Schmidt, J. Bernholc, A. M. Frisch, P. Vogt, M. Zorn, M. Pristovsek, W. Richter, F. Bechstedt, T. Hanappel, and S. Visbeck, J. Vac. Sci. Technol. B **17**, 1691 (1999).
[15] W. G. Schmidt, S. Mirbt, and F. Bechstedt, Phys. Rev. B **62**, 8087 (2000).
[16] C. Ratsch, W. Barvosa-Carter, F. Grosse, J. H. G. Owen, and J. J. Zinck, Phys. Rev. B **62**, R7719 (2000).
[17] F. Maeda, Y. Watanabe, and M. Oshima, Phys. Rev. B **48**, 14733 (1993).
[18] R. Ludeke, T.-C. Chiang, and D. E. Eastman, Physica B **117&118**, 819 (1983).
[19] G. Le Lay, D. Mao, A. Khan, Y. Hwu, and G. Margaritondo, Phys. Rev. B **43**, 14301 (1991).
[20] I. M. Vitomirov, A. Raisanen, A. C. Finnefrock, R. E. Viturro, L. J. Brillson, P. D. Kirchner, G. D. Pettit, and J. M. Woodall, Phys. Rev. B **46**, 13293 (1992).
[21] M. Sugiyama, S. Maeyama, F. Maeda, and M. Oshima, Phys. Rev. B **52**, 2678 (1995).
[22] T.-L. Lee and M. J. Bedzyk, Phys. Rev. B **57**, R15056 (1998).
[23] P. Moriarty, P. H. Beton, Y.-R. Ma, M. Henini, and D. A. Woolf, Phys. Rev. B **53**, R16148 (1996).
[24] L. J. Whitman, B. R. Bennett, E. M. Kneedler, B. T. Jonker, and B. V. Shanabrook, Surf. Sci. **436**, L707 (1999).
[25] N. Esser, A. I. Shkrebtii, U. Resch-Esser, C. Springer, W. Richter, W. G. Schmidt, F. Bechstedt, and R. Del Sole, Phys. Rev. Lett. **77**, 4402 (1996).
[26] W. G. Schmidt and F. Bechstedt, Phys. Rev. B **55**, 13051 (1997).
[27] F. Maeda, Y. Watanabe, and M. Oshima, Surf. Sci. **357–358**, 540 (1996).
[28] P. K. Larsen, J. F. van der Veen, A. Mazur, J. Pollmann, J. H. Neave, and B. A. Joyce, Phys. Rev. B **26**, 3222 (1982).
[29] M. T. Sieger, T. Miller, and T.-C. Chiang, Phys. Rev. B **52**, 8256 (1995).
[30] L. J. Whitman, P. M. Thibado, S. C. Erwin, B. R. Bennett, and B. V. Shanabrook, Phys. Rev. Lett. **79**, 693 (1997).
[31] P. M. Thibado, B. R. Bennett, B. V. Shanabrook, and L. J. Whitman, J. Cryst. Growth **175/176**, 317 (1997).
[32] F. Maeda and Y. Watanabe, Phys. Rev. B **60**, 10652 (1999).
[33] M. Naganuma, S. Miyazawa, and H. Iwasaki, J. Vac. Sci. Technol. **17**, 606 (1980).
[34] J. J. Zinck, E. J. Tarsa, B. Brar, and J. S. Speck, J. Appl. Phys. **82**, 6067 (1997).
[35] D. E. Eastman, T.-C. Chiang, P. Heimann, and F. J. Himpsel, Phys. Rev. Lett. **45**, 656 (1980).
[36] L. Ö. Olsson, J. Kanski, L. Ilver, C. B. M. Andersson, M. Björkqvist, M. Göthelid, U. O. Karlsson, and M. C. Håkansson, Phys. Rev. B **50**, 18172 (1994).

[37] L. Ö. Olsson, L. Ilver, J. Kanski, P. O. Nilsson, C. B. M. Andersson, U. O. Karlsson, and M. C. Håkansson, Phys. Rev. B **53**, 4734 (1996).

[38] P. K. Larsen, J. H. Neave, J. F. van der Veen, P. J. Dobson, and B. A. Joyce, Phys. Rev. B **27**, 4966 (1983).

[39] J. F. van der Veen, P. K. Larsen, J. H. Neave, and B. A. Joyce, Solid State Commun. **49**, 659 (1984).

[40] M. D. Pashley, Phys. Rev. B **40**, 10481 (1989), and references therein.

[41] T.-C. Chiang, R. Ludeke, M. Aono, G. Landgren, F. J. Himpsel, and D. E. Eastman, Phys. Rev. B **27**, 4770 (1983).

[42] T.-C. Chiang, J. A. Knapp, M. Aono, and D. E. Eastman, Phys. Rev. B **21**, 3513 (1980).

[43] M. C. Håkansson, L. S. O. Johansson, C. B. M. Andersson, U. O. Karlsson, L. Ö. Olsson, J. Kanski, L. Ilver, and P. O. Nilsson, Surf. Sci. **374**, 73 (1997).

[44] W. R. A. Huff, M. Shimomura, N. Sanada, G. Kaneda, T. Takeuchi, Y. Suzuki, H. W. Yeom, T. Abukawa, S. Kono, and Y. Fukuda, Phys. Rev. B **57**, 10132 (1998).

[45] W. G. Schmidt and F. Bechstedt, Phys. Rev. B **54**, 16742 (1996).